Hydrology and
Earth System
Sciences

The role of land and ocean evaporation on the variability of precipitation in the Yangtze River valley

Astrid Fremme and Harald Sodemann

Geophysical Institute, University of Bergen, and Bjerknes Centre for Climate Research, Bergen, Norway

Correspondence: Astrid Fremme (astrid.fremme@uib.no)

Abstract. The Yangtze River valley (YRV) experiences large intraseasonal and interannual precipitation variability, which is mainly due to East Asian monsoon influence. The East Asian monsoon is caused by interaction of many processes in the coupled land–atmosphere–ocean system. To better understand YRV precipitation variability in this complex system, we have studied the precipitation moisture sources and their connection to YRV precipitation. We obtained the moisture sources by using the European Centre for Medium-Range Weather Forecasts' (ECMWF) ERA-Interim reanalysis dataset, the FLEXible PARTicle dispersion model (FLEXPART), and the WaterSip moisture source diagnostic. The variability of moisture sources reflects the variability of YRV precipitation. Intraseasonal variations of moisture sources include a shift of the most important source regions as the monsoon progresses. Interannual variability of the moisture sources shows that sources which are less important climatologically are closely connected to variations of the driest and wettest years. Our results show that land directly contributes 58 % of moisture for YRV precipitation during 1980–2016, whereas the ocean contributes 42 % in direct transport. While the importance of the ocean as a moisture source is often emphasized, our results underscore the importance of the process of continental recycling and the role of land moisture sources.

1 Introduction

The Yangtze River valley (YRV) lies on the east coast of China. The region is affected by the East Asian monsoon and experiences dry winters and wet summers. Winters are dominated by cold and dry winds from continental regions to the northwest, while summer circulation is characterized by substantially more warm and moist southwesterly winds which bring the monsoon precipitation to the YRV (Huang et al., 2012). The focus of this study is on the wettest half of the year, namely, the months of April to September, in which the YRV receives 72 % of its annual precipitation.

The population of the YRV in East China depends on monsoon rainfall for agriculture and water supply. At the same time, variability of monsoon rainfall can have negative consequences through droughts and floods (Huang et al., 2007; Piao et al., 2010). The mechanisms causing rainfall variability are not fully understood, and future changes in precipitation are uncertain (Sun et al., 2016). A continued search for a better understanding of the processes causing rainfall variability therefore remains vital.

The East Asian monsoon precipitation exhibits variability regarding different aspects. The monsoon varies in its onset, rainfall amount, and spatial distribution (Ding and Chan, 2005). Being situated in a humid region, precipitation variability in the YRV is mostly connected to flood episodes. In 1998, for example, regions along the Yangtze River experienced extraordinarily heavy floods, with on average 9.1 mm d^{-1} summer rainfall during that year (Jun and Chen, 2001). On the other hand, the driest summer since 1979 was the year of 2005, with an average of 4.4 mm d^{-1}. Variability of the East Asian monsoon is characterized by the interaction of many processes in the coupled land–atmosphere–ocean system. Some of these are the variability and strength of the monsoon circulation, the temperature of the surrounding oceans, the persistence of the Meiyu front, and the position of the Western Pacific Subtropical High (WPSH; Ding and Chan, 2005; Feng et al., 2015).

The variability of moisture sources for a precipitation event can be affected by changes in factors such as evaporation and moisture transport or precipitation-causing mechanisms. The variability of moisture sources may be directly linked to precipitation variability but at the same time result from changes in other factors. In this study we seek to identify and understand factors contributing to intraseasonal precipitation variability from such a moisture source perspective.

One of the prime factors that have been investigated as mechanisms behind precipitation variability is the variability of moisture contribution from the surrounding oceans. Since moisture origin is not a directly observable quantity, indirect, model-based methods have been used to determine the variation of this factor.

Studies with an emphasis on finding oceanic moisture sources have located and quantified the most important ocean regions such as the Arabian Sea and the Bay of Bengal (BoB) as parts of the northern Indian Ocean, the South China Sea (SCS), and the East China Sea as part of the Western Pacific (Zhou and Yu, 2005; Zhou et al., 2010; Wang and Chen, 2012; Chen et al., 2013). Zhou and Yu (2005), for example, examine water vapor transport patterns corresponding to different positions of the main rain belt over East China. They found that the rain belt pattern associated with rainfall over the YRV receives moisture from midlatitude northeast water vapor as well as tropical southwest water vapor from BoB and SCS which can be traced back to the Philippine Sea. Zhou et al. (2010) found that the majority of moisture inflow to eastern China comes through the northern boundary of the SCS with 200×10^6 kg s^{-1} through this boundary. In their results an inflow of 152×10^6 kg s^{-1} over a boundary at $100°$ E also suggests that land sources can play an important role for East China.

More recently the role of land regions as moisture sources to YRV has been more strongly recognized (Wei et al., 2012; Sun and Wang, 2015; Zhao et al., 2016; Rodríguez et al., 2017; Pan et al., 2017; Li et al., 2016; Drumond et al., 2011). Previous studies have used a range of different methods, and as a result, the location of key moisture sources varies between studies. While some studies find land sources to be spread out over large regions (Wei et al., 2012; Sun and Wang, 2015; Zhao et al., 2016; Rodríguez et al., 2017; Pan et al., 2017), others emphasize the YRV region itself as the strongest land source (Li et al., 2016; Drumond et al., 2011). Wei et al. (2012) found that the most important moisture sources mainly lie in the pathways for moisture transport over land and that the ocean plays an important role in initiating the transport. Local evapotranspiration in a region similar to the YRV accounts for about 10 %–15 % during the wet season, while Indochina contributes 8 %–15 %, South China 13 %–15 %, Western Pacific 5 %–15 %, SCS 6 %–12 %, and BoB 3 %–11 %. Indochina, South China, and the BoB are the most important moisture sources during the precipitation peak of the monsoon. Pan et al. (2017) found that the

BoB and Arabian Sea contribute < 4 % during summer. They found the northwestern Pacific to be the dominant oceanic source to YRV in other months (15.8 %–24.6 %) than June and July (8.1 %–10.6 %). In June and July the northern Indian Ocean was the dominant oceanic source region with a contribution of ∼ 30 %. The Indochina Peninsula contributed ∼ 9.9 % of annual precipitation. Local YRV evaporation and South China had a combined contribution in summer exceeding 10 %.

According to these latter studies, moisture contribution from the land surface provides an important fraction of the monsoon precipitation. The land surface provides moisture to the YRV through recycling of moisture from previous precipitation events. We use the term continental recycling for moisture recycling from any land region, while the term local recycling refers to recycling within the target region. During recycling events moisture originates from and interacts with the land surface. Disregarding moisture recycling can impact our view of moisture sources to YRV and their variability. Moisture recycling should be kept in mind when searching for possible mechanisms affecting the monsoon precipitation.

The lack of agreement with respect to both location and magnitude of the moisture sources for the YRV highlights the need for further attempts to locate the spatial distribution of moisture sources to the YRV, the moisture contributions from land and ocean, and the seasonal cycle of the moisture sources. We apply here the state-of-the-art Lagrangian moisture source diagnostic of Sodemann et al. (2008), which provides a quantitative accounting of the contributions of evaporation along the flow path of air masses precipitating in a predefined target area.

Baker et al. (2015) used the same diagnostic over a large region of China for a 5-year period. In their study, the main focus was linking moisture source variations to the stable water isotope composition in cave deposits. Our present study, in contrast, examines the moisture sources of a more focused domain with relatively homogeneous precipitation regime. We first aim at finding robust features of the moisture source distribution and intraseasonal to interannual variability, covering a 37-year period. Next, we estimate the sources beyond the direct moisture contribution, exploring land and ocean moisture sources further back in time. Lastly, we explore local factors which might affect moisture sources and precipitation, before drawing our conclusions.

2   Method and data

For this study we use a Lagrangian method to identify moisture sources to the Yangtze River valley. Lagrangian methods follow the movement of air parcels through the atmosphere over time (Stohl et al., 1998; Stohl and Thomson, 1999). The humidity budget of an air parcel can be modified by evapotranspiration and precipitation as the air mass moves around

the atmosphere. In a Lagrangian perspective, these quantities are denoted as e and p respectively (Stohl and James, 2004):

$$\Delta q = e - p, \tag{1}$$

where Δq is the change in specific humidity of an air parcel over a 6 h time period.

Different methods are in use to identify the moisture sources from trajectories. Here we use the Lagrangian moisture source diagnostic WaterSip (Sodemann et al., 2008). The WaterSip method assumes that for each 6 h time step either e or p will dominate while the other can be disregarded. Increases in specific humidity in the air parcels exceeding a threshold value Δq_c are thus taken to be due to evaporation or transpiration from the surface, whereas decreases are due to precipitation. Data on evaporation and precipitation are not used directly but rather estimated by Δq. Trajectories of air parcels precipitating over the target region are evaluated individually. Starting at 15 d before a precipitation event, at each time step, the fractional contribution of a humidity increase (thought to be due to dominating evaporation) to the previous specific humidity of the air parcel at that time is calculated. In case of precipitation, previous evaporation regions are assumed to contribute according to the fraction they represent in the air parcel.

When part of the humidity of an air parcel precipitates, all earlier contributions contribute and are thereby discounted. For example, a mass of moisture originally gained by the air parcel 10 days before reaching the target region might all be lost to precipitation the next day, still several days before reaching the target region. In this case, the earlier uptake and its region will no longer be counted as a source for subsequent precipitation events by the air parcel.

This so-called moisture accounting provides a fractional contribution of each evaporation event to the final precipitation in the target area. Furthermore, it provides the percentage of the precipitation for which moisture sources have been identified. Notably, the method does not critically depend on the length of trajectories beyond a certain number of days. Due to the accounting method, expanding the analysis period from 10 to 20 d, for example, typically only results in the identification of an additional 5 %–10 % of the moisture sources (Sodemann and Stohl, 2009). This particular property of the method contrasts with the widely used Lagrangian $e - p$ method (Stohl and James, 2004). There, the net effect of $e - p$ events for the air parcel trajectories is aggregated over a predefined time period, and results depend on the chosen aggregation period (e.g., Stohl et al., 2008).

The WaterSip diagnostic tool is also used to obtain the so-called second-order moisture sources. This measure gives us more information on the number of times moisture goes through precipitation and re-evaporation over land before reaching the target region. Obtaining the second-order moisture sources is a three-step process in addition to obtaining the YRV moisture sources. Firstly, the moisture sources to a larger region of Asia are calculated, and the land fraction

to the Asian region is obtained. This land contribution fraction is found by analyzing each trajectory separately. Knowing the moisture sources and relative contribution to each precipitation event, the land fraction is calculated. Secondly, the monthly mean land fraction over the Asian region is obtained by weighting by the contribution from each trajectory to precipitation over the region. For the third step we assume that continental moisture originates from precipitation in the same region within the same month. Folding the YRV land moisture sources by the fraction of land contribution to the source regions then gives the second-order moisture source land fraction to the YRV.

We use the air parcel trajectory dataset of Läderach and Sodemann (2016) as a basis for the Lagrangian diagnostic WaterSip, which has been extended by 3 years and now covers the period 1980–2016. The dataset has been calculated using the Lagrangian particle dispersion model FLEXPART V8.2 (FLEXible PARTicle dispersion model; Stohl et al., 2005), using the 6-hourly European Centre for Medium-Range Weather Forecasts' (ECMWF) ERA-Interim reanalysis (Dee et al., 2011). ERA-Interim (Dee et al., 2011) has been shown to be the best reanalysis dataset for representing monsoon precipitation (Lin et al., 2014; Huang et al., 2016). It is in good agreement with observations over monsoon regions and specifically also over eastern China (Liu et al., 2018). The trajectory dataset of Läderach and Sodemann (2016) represents the global atmosphere by 5 million air parcels of equal mass. Trajectories contain the horizontal and vertical position and specific humidity along with other atmospheric variables (see Läderach and Sodemann, 2016, for further details). Trajectories are first extracted for all air parcels precipitating over the target region before the WaterSip method described above is applied.

The analysis region for the YRV spans 27–33° N and 110–122° E (Fig. 1, red box). We focus on the lower valley only, not including to the upper reaches of the Yangtze River basin (west of 110° E), which experience a different precipitation regime (Chen et al., 2009).

The target region is limited to land areas with a threshold of 25 m minimum elevation. Other thresholds for the moisture source diagnostic are 0.1 g kg^{-1} for Δq_c, a trajectory length of 15 d, and relative humidity > 80 % for precipitation over the YRV. No distinction is made for moisture uptake within and above the boundary layer. These thresholds lead to a good representation of the spatial distribution and the seasonal cycle of precipitation over the YRV (Fig. 2). The thresholds result in source attribution for 95 % of the WaterSip precipitation.

As part of this study, monthly ERA-Interim data for soil moisture, evaporation, and 850 hPa wind are used for direct comparison with moisture source results. For comparison with vegetation we include the normalized difference vegetation index (NDVI). For the NDVI we use the 1982–2015 monthly average of the satellite-observed third-generation NDVI from the National Oceanic and Atmo-
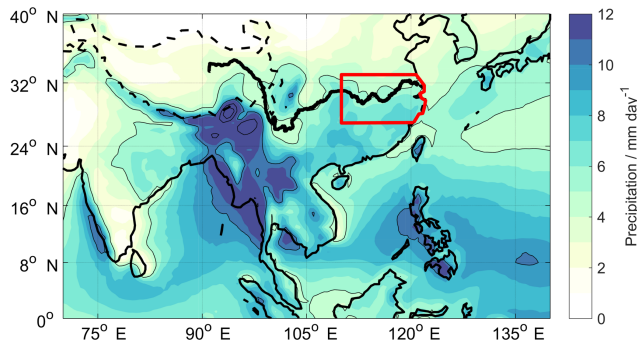
Figure 1. ERA-Interim precipitation (shading) over South and East Asia in millimeters per day ($mm\,d^{-1}$). Black contours are shown every $5\,mm\,d^{-1}$. The YRV target region (red), the Yangtze River (black), and the 4 km topography contour of the Tibetan Plateau (dotted line) are shown. Precipitation is the 1980–2016, April–September mean.

spheric Administration's (NOAA) Advanced Very High Resolution Radiometer (AVHRR) (Pinzon and Tucker, 2014).

For validation, ERA-Interim precipitation is compared to precipitation in the gridded observational dataset CN05.1 (Wu and Gao, 2013), which is based on observations in China. This dataset is used for the years 1980–2014. The result of this comparison is presented in the next section.

3　Data and method validation

The climatological precipitation in East Asia

Precipitation over South and East Asia in the ERA-Interim dataset has a maximum at the southern edge of the Tibetan Plateau and at the eastern border of the Bay of Bengal during April–September (Fig. 1). While large regions receive more than $10\,mm\,d^{-1}$ between April and September, the target region of this study, the lower reaches of the Yangtze River, denoted here as the Yangtze River valley, receives on average $5.9\,mm\,d^{-1}$ of precipitation (Fig. 1, red box). YRV wet season precipitation shows a meridional gradient, with $4\,mm\,d^{-1}$ in the north and up to $8\,mm\,d^{-1}$ in the south (Fig. 2a). ERA-Interim's representation of precipitation shows a similar spatial pattern as the high-resolution, gridded observational dataset CN05.1 (Wu and Gao, 2013) (Fig. 2a and b). The spatial pattern of precipitation obtained through the WaterSip method described in Sect. 2 is also similar (Fig. 2c).

The YRV has a pronounced precipitation seasonality. The six wettest months are April to September, and precipitation peaks in June (Fig. 2d). Both June and July are considered peak monsoon months (Ding and Chan, 2005). The monsoon precipitation and overall precipitation seasonality agree well between the reanalysis, observations, and estimated from the WaterSip method (Fig. 2d), with on aver-

age 5.9, 5.9, and $5.2\,mm\,d^{-1}$ respectively. The similarity in both patterns, amount, and seasonal cycle of precipitation validates the use of the WaterSip method for this region. While there is an overestimation during most months of the year, WaterSip underestimates ERA-Interim precipitation in summer (JJA) with an average of 20.5 %. Of the precipitation estimated by the WaterSip method, 95 % is attributed to a source, while 5 % is not accounted for, for example due to moisture sources further back in time than 15 d. The remainder of this study is only based on the moisture that can be attributed to a source.

4　Results

### 4.1　Climatological mean moisture sources of YRV precipitation

For each precipitation event in the YRV during the ERA-Interim period, we trace back to the moisture sources using the WaterSip method. The resulting average moisture sources for the YRV in April–May are shown in Fig. 3a. The shading can be interpreted as the contribution of evaporation to YRV precipitation in units of millimeters per day ($mm\,d^{-1}$), equivalent to kilograms per square meter per day ($kg\,m^{-2}\,d^{-1}$). Moisture contributions range from $0\,mm\,d^{-1}$ in white to $1\,mm\,d^{-1}$ in black. The maximum contribution is from southwest China, while large parts of Asia and the surrounding oceans contribute only small amounts. The 50th and 80th percentiles enclose 50 % and 80 % of the total moisture contribution by picking the grid points with largest contributions (Fig. 3a–c, dashed red lines). The extent of the percentiles denote the most important source regions. At the same time, the region between both red lines shows the importance of relatively moderate contributions spread out over a large area, contributing 30 % of the moisture.

Through the course of the wet season, the most intense source region to the YRV gradually moves closer and more northeast as the monsoon progresses (Fig. 3a–c). At the start of the wet season, in April–May, the most pronounced source regions are over the western part of South China and the Indochina Peninsula (Fig. 3a). In June–July the eastern part of South China becomes more important (Fig. 3b), and by August–September East China becomes the dominant moisture source to YRV (Fig. 3c). The largest source contributions for the 2-month climatologies are during June–July, when the sum of the moisture source contributions provide the YRV precipitation maximum. The mean precipitation in the YRV during June–July is $7.1\,mm\,d^{-1}$ (Fig. 2d), with maxima of $8.8\,mm\,d^{-1}$ in the south and west in the region (not shown). The overall maximum source is then over South China (Fig. 3b), with $0.97\,mm\,d^{-1}$.

The 80th percentiles show equally pronounced changes (Fig. 3a–c). In April–May the 80th percentiles cover mostly land regions, the South China Sea, and small parts of the
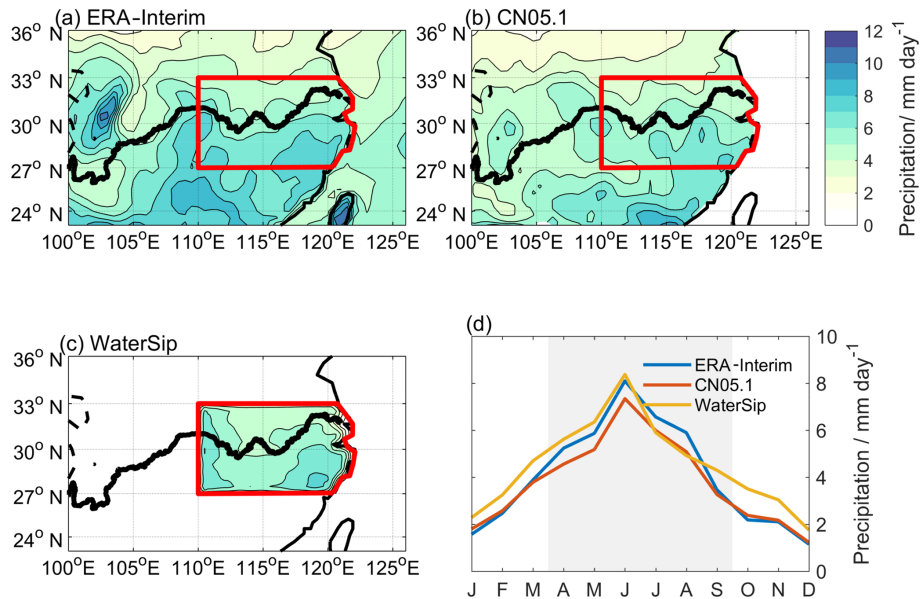
Figure 2. Precipitation over the YRV target region. April–September mean according to **(a)** ERA-Interim, **(b)** the gridded observational dataset CN05.1, and **(c)** values estimated by the WaterSip method. **(d)** shows monthly precipitation over the YRV region for ERA-Interim, CN05.1, and WaterSip. ERA-Interim and WaterSip climatologies are for 1980–2016, while the CN05.1 climatology is for 1980–2014. Units are millimeters per day (mm d^{-1}).
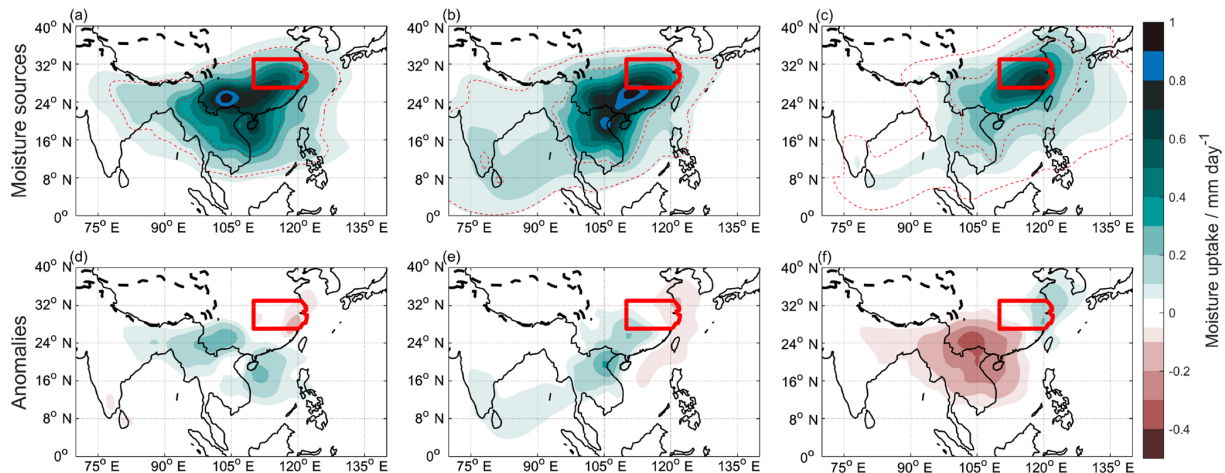
Figure 3. Two-month mean moisture sources for YRV for April–September. **(a–c)** show the mean moisture sources for **(a)** late spring (April–May), **(b)** midsummer (June–July), and **(c)** extended late summer (August–September). The lower panels show the **(d)** April–May, **(e)** June–July, and **(f)** August–September anomalies compared to the April–September mean. The target region (red) and 4000 m elevation of the Tibetan Plateau (dotted contour) are shown. The 50th and 80th percentiles of the mass contributed from moisture sources are shown in red dotted contours **(a–c)**. The units are millimeters per day (mm d^{-1}).

Western Pacific. In June–July the 80th percentile stretches out over India and the Indian Ocean, while in August–September it shifts further into the Western Pacific. The contribution from weaker moisture sources corresponds to the area between the 50th and 80th percentiles. The region between the two percentiles is the source for 30 % of the moisture, with a contribution below 0.2 mm d^{-1} in June–July.

Comparing each 2-month period to the overall wet season mean we obtain the 2-month anomalies (Fig. 3d–f). These anomalies are shown with green (red) values for above (below) average contribution. The anomalies highlight the northward and eastward movement of the most important sources through the wet season. In April–May (Fig. 3d) the southwestern edge of China and Myanmar contribute more than average, together with the South China Sea. In June–

July (Fig. 3e) the Bay of Bengal, Indochina Peninsula, and South China contribute more than average. At the end of the wet season, in August–September (Fig. 3f), eastern China and the Yellow Sea are the only regions that contribute more than average. The reason for the high uptake within the YRV region in August–September is investigated further in Sect. 4.5. During August–September, the South China continental areas, the Indochina Peninsula, and the South China Sea all contribute less than for the preceding wet months.

Changes in the total contribution from all source regions are directly reflected in precipitation amount over the YRV. Variability in moisture sources is thus intimately connected to variability of YRV precipitation. The YRV moisture sources show large seasonal variations, reflecting the large seasonal precipitation variations.

The distribution of moisture sources for the YRV found here generally agrees with a range of previous studies (Wei et al., 2012; Sun and Wang, 2015; Zhao et al., 2016; Rodríguez et al., 2017; Pan et al., 2017; Baker et al., 2015). However, our results are also in disagreement with studies focusing exclusively on oceanic moisture sources (Zhou and Yu, 2005; Wang and Chen, 2012; Chen et al., 2013; Zhou et al., 2010) or studies using the $e - p$ method (Li et al., 2016; Drumond et al., 2011). The results of this study are not necessarily in a direct contradiction to previous work, as there are different views on the effect which land recycling and the evaporation of moisture for precipitation has on the definition of moisture sources. Furthermore, each method for studying moisture sources is associated with uncertainties. An advantage of the WaterSip method is that, instead of dealing with values for p and ET obtained from model parametrization, these variables are estimated through more observation-restrained humidity changes in the atmosphere. As a first-order result, the similarities to a range of previous studies using very different methods are encouraging. The results of this study are then further compared in more detail to the literature in Sect. 5.

4.2 Mean seasonal cycle of YRV moisture sources

The YRV moisture sources for April–September show temporal changes, both with respect to location and amount. To examine the changes and the seasonal progression in more detail, we subdivide moisture sources into six land and four ocean regions (Fig. 4). The monthly climatology of the contribution from each region shows pronounced seasonality in all regions (Fig. 5).

In Fig. 5 the peak contribution of all regions ranges from 3.5 to 8×10^{11} kg d^{-1}, which corresponds to 0.37 and 0.82 mm d^{-1}, respectively, if distributed evenly over the YRV region.

The spread of moisture contributions in Fig. 5 shows the interannual standard deviation of the moisture contributed from each source region. The regions with the largest standard deviation are the South China Sea (Fig. 5d) and the
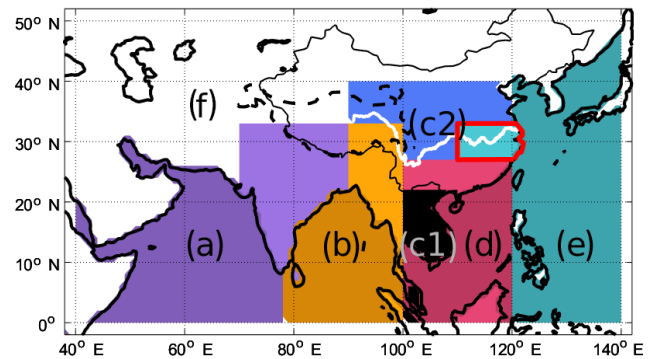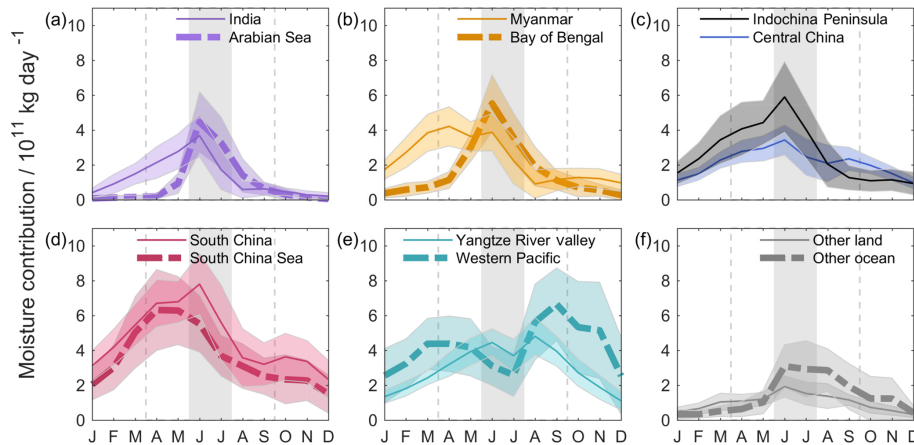

Figure 4. Definition of source regions. The different regions are named (a) Arabian Sea and India, (b) Bay of Bengal and Myanmar, (c1) Indochina Peninsula, (c2) Central China, (d) South China Sea and South China, (e) Western Pacific and the target region of the lower Yangtze River valley, and (f) remaining ocean and land regions. The target region (red) and 4000 m elevation of the Tibetan Plateau (dotted contour) are shown.

Table 1. Moisture source contribution fraction to the Yangtze River valley (YRV) in percent. Averages are weighted by monthly contribution.

	April–May	June–July	August–September	Wet season mean
Land sources				
India	6.3 %	6.0 %	2.2 %	5.2 %
Myanmar	10.1 %	6.8 %	3.7 %	7.2 %
Indochina Peninsula	10.9 %	11.0 %	5.8 %	9.6 %
Central China	7.4 %	6.6 %	7.8 %	7.2 %
South China	17.3 %	14.9 %	11.9 %	14.9 %
Yangtze River valley	9.1 %	9.0 %	15.4 %	10.7 %
Remaining land regions	3.0 %	3.9 %	4.5 %	3.7 %
Land sources total	64.0 %	58.1 %	51.2 %	58.4 %
Ocean sources				
Arabian Sea	1.5 %	8.6 %	3.6 %	4.9 %
Bay of Bengal	5.3 %	10.1 %	5.3 %	7.2 %
South China Sea	16.1 %	10.2 %	9.9 %	12.2 %
Western Pacific	11.0 %	6.3 %	21.5 %	11.7 %
Remaining ocean sources	2.1 %	6.7 %	8.4 %	5.5 %
Ocean sources total	36.0 %	42.0 %	48.8 %	41.6 %

Western Pacific (Fig. 5e). The role of these and other sources regarding interannual variability and their connection to dry and wet years is explored further in Sect. 4.6.

Another feature of Fig. 5 is the timing of contribution from the different moisture sources. For spring and the pre-monsoon season (April–May), the South China Sea (Fig. 5d), South China (Fig. 5d), and the Myanmar region (Fig. 5b) are important moisture sources. They provide 16.1 %, 17.3 %, and 10.1 % respectively (Table 1). Combined, this moisture contributes a substantial fraction of the pre-monsoon precipitation (43.5 %).

Figure 5. Moisture contribution from different source regions. Division and colors correspond to those in Fig. 4. Thick dashed lines show oceanic regions, while thin continuous lines show continental regions. The wettest half of the year is marked, with peak-precipitation months June and July shaded. Contribution and standard deviation of contribution are shown for the different regions: **(a)** Arabian Sea and India, **(b)** Bay of Bengal and Myanmar, **(c1)** Indochina Peninsula, **(c2)** Central China, **(d)** South China Sea and South China, **(e)** Western Pacific and the target region of the lower Yangtze River valley, and **(f)** remaining ocean and land regions. The units are 10^{11} kg d^{-1}.

During the monsoon precipitation peak months of June–July, contributions from the distant westernmost moisture sources of the Bay of Bengal (Fig. 5b), India (Fig. 5a), and the Arabian Sea (Fig. 5a) show pronounced peaks. This coincides with the strong westerlies of the Indian monsoon and provides a link between the Indian and East Asian monsoons. These short-term, distant sources contribute 10.1 %, 6.0 %, and 8.6 % respectively in June–July (Table 1), a combined 24.7 % of the total June–July moisture contribution. During June–July a peak in contribution can also be seen for the Indochina Peninsula (Fig. 5c) and South China (Fig. 5d), although these regions also contribute substantially in spring. These two land regions contribute 11.0 % and 14.9 % in June–July (Table 1). The two land regions lie in the path of moisture arriving at the YRV from the Indian Ocean. We hypothesize that moisture transported from the Indian Ocean, which precipitates and re-evaporates on its way to the YRV, will have the en-route land regions as new moisture sources. This will be further investigated in Sect. 4.4.

For the late part of the monsoon, during August–September, the Western Pacific and the YRV region itself (Fig. 5e) become more important. During August–September these regions contribute 21.5 % and 15.4 % respectively (Table 1). This is a time when the region also experiences a decrease in moisture contribution from all other moisture source regions, suggesting a changeover of moisture transport mechanisms in the monsoon system. This important transition period is further investigated in the next section (Sect. 4.3).

Regarding the causes of YRV precipitation variability, we note that different source regions are responsible for providing moisture for precipitation in the different stages of the monsoon. It is therefore conceivable that different mecha-

nisms, such as continental recycling or long-range moisture transport, can play a role at different stages of the monsoon.

4.3 Continental recycling and regional evaporation recycling in the YRV

During the summer months, the YRV receives almost equal contributions from land and ocean sources. For the April–September wet season months, land sources contribute 58.4 % of moisture for YRV precipitation while the ocean sources contribute 41.6 % (Table 1). We refer here to contributions from land sources as *continental recycling* (Goessling and Reick, 2011). This term has a wider perspective than *local recycling*, which only includes continental recycling from within the YRV (see Sect. 4.5). Continental recycling varies between 66 % in February and 51 % in August (Fig. 6). With more than half of the moisture provided through continental recycling, this mechanism appears as important in sustaining YRV humidity and precipitation during the wet season.

Previous studies which considered land contributions to YRV precipitation reported between 30 % and 60 % continental recycling for different seasons and slightly different target regions, with a gradient of lower continental recycling to the southeast in the region and more land contributions to the northwest (Sun and Wang, 2015; Zhao et al., 2016; Pan et al., 2017). As studies used different regions and time periods, continental recycling values are not directly comparable. The continental recycling fraction found in this study is nonetheless higher than what was found in previous studies. To further investigate the plausibility of this result, we compare moisture contribution from continental recycling to the total evapotranspiration (ET) due to the land surface and vegetation.
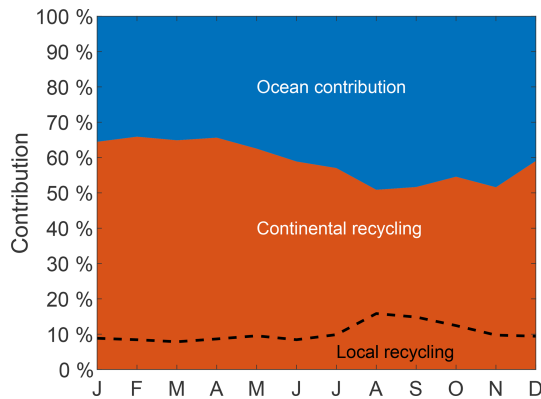
Figure 6. Fraction of land and ocean contribution to YRV precipitation. Local recycling is shown with a dashed line and is a subset of continental recycling.

ERA-Interim mean ET over South and East Asia in April–September shows a meridional gradient, with about $3–4\,\mathrm{mm\,d^{-1}}$ in the south and below $1\,\mathrm{mm\,d^{-1}}$ in the north (Fig. 7a). Ocean evaporation is stronger, with maxima of over $5\,\mathrm{mm\,d^{-1}}$ in the Bay of Bengal and Arabian Sea. ET values are generally lower, but the pattern resembles that of precipitation over the same regions (Fig. 2a).

While the ET displayed in Fig. 7a suggests a dominating role of the oceans, our analysis highlights that moisture source contributions to the YRV are only a subset of ET at the moisture source regions. The fraction ϵ of ET that ultimately arrives as precipitation in the YRV is calculated as

$$\epsilon = \frac{ET_{YRV,P}}{ET_{TOT}}, \tag{2}$$

where $ET_{YRV,P}$ is the amount contributed from the moisture source to YRV precipitation, and ET_{TOT} is the total ET. The ϵ within the YRV region is sometimes referred to as the regional evaporation recycling ratio (van der Ent et al., 2014), which shows the ratio of ET that subsequently precipitates within the same region.

For the April–September mean ϵ is mostly below 50 % (Fig. 7b) for all source regions. Values over South China are the highest, where more than 40 % of ET in some regions results as YRV precipitation. The highest values over the ocean appear over the Western Pacific by the Yangtze River outlet and the South China Sea by the Indochina Peninsula. The values of Fig. 7b underline that ET is clearly sufficient to fuel the moisture sources obtained in this study. This underlines the plausibility of the continental recycling values found in this study and our moisture source results in general.

4.4 Second-order moisture sources of recycled precipitation

YRV precipitation provided through continental recycling can itself have a local or remote origin. In this section we examine the sources of moisture from continental recycling arriving at the YRV, found according to the description in Sect. 2

We start out with the continental moisture sources to YRV previously identified from the WaterSip method (Fig. 8a). Next, we calculate the local fraction of continental recycling for a larger region encompassing South, East, and Central Asia (Fig. 8b). The Asian continental recycling fraction shows a north-to-south gradient of decreasing continental recycling, coinciding with an increasing gradient with distance from the coast. Multiplication of the YRV moisture sources (Fig. 8a) and the Asian continental recycling fraction (Fig. 8b) yields the contribution of land sources to precipitation from continental sources to the YRV, termed here the second-order continental moisture sources (Fig. 8c). In this calculation, monthly averages were used to allow for a possible lag between precipitation and re-evaporation. While Fig. 8c does not show the regional extent of the second-order moisture sources, it does provide information on the amount of YRV moisture which still has continental origin even before the last continental recycling event.

These results show that about two-thirds (in summer) to three-fourths (in winter) of the land source contributions to YRV have their origin over land, while one-third (in summer) to one-fourth (in winter) comes from the ocean. In combination with earlier results on the direct land and ocean contribution to YRV, this implies that the YRV has 41.6 % of the direct ocean contribution for April–September precipitation and 17.6 % of continental recycling which is ocean contribution recycled once on land, while the remaining 40.8 % of moisture to YRV has been recycled over land at least twice (Table 2).
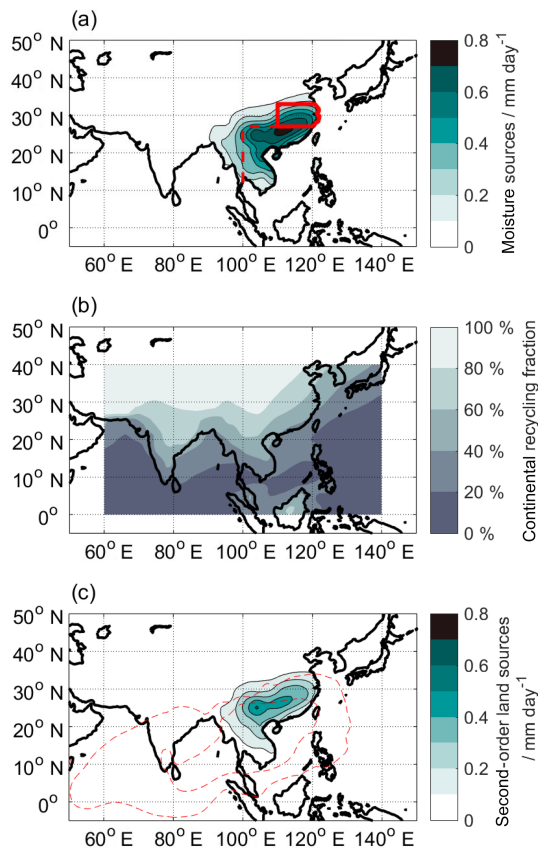
South China and the Indochina Peninsula (Fig. 8a, dashed red lines) are the two most important exterior continental moisture sources of the YRV, contributing about 24 % of summer precipitation. As already highlighted in Sect. 4.2, the June–July peak of the Indochina Peninsula and South China moisture contribution might be connected to moisture transport from the Indian Ocean, precipitating and re-evaporating en route to the YRV. The 50th and 80th percentiles of the moisture sources for that region as a whole extend over South and East Asia, the surrounding oceans, and India (Fig. 8c, dashed red lines). The sources for South China and the Indochina Peninsula are therefore examples of important second-order sources of the YRV.

An advantage of the approach used here is the ability to quantify the degree to which moisture undergoes multiple recycling events (see Sect. 2). The second-order continental sources show how moisture can be traced further back, sometimes back to when it evaporated from the ocean. Our results for the second-order sources emphasize the importance of the ocean in providing moisture which eventually undergoes continental recycling. They also reveal the substantial fraction (40.8 % in April–September) which is recycled on land more than once. Regarding the variability of the mon-
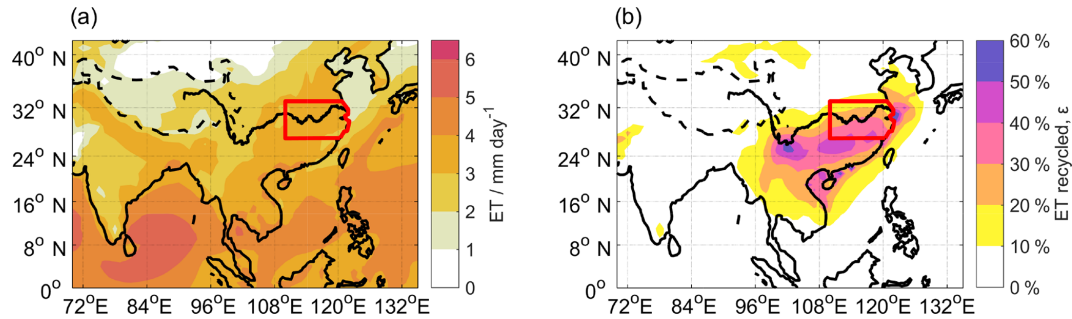
Figure 7. Evapotranspiration **(a)** and ϵ, the fraction of evapotranspiration resulting as YRV precipitation **(b)**. The values are the April–September, 1980–2016 means. ET data are from ERA-Interim and in millimeters per day (mm d^{-1}), while ϵ is a combination of WaterSip results and ET.

Figure 8. Identification of second-order land sources. Continental moisture sources to YRV are shown in millimeters per day (mm d^{-1}) **(a)**, with the YRV as a red box and the combined region of South China and the Indochina Peninsula demarcated by dashed red lines. **(b)** shows the fraction of continental recycling to a larger section of Asia. **(c)** shows in shading the second-order land contribution in millimeters per day (mm d^{-1}) to YRV, which is the product of **(a)** and **(b)**, and in dashed red lines the 50th and 80th percentiles of moisture sources to South China and the Indochina Peninsula.

soon precipitation in the YRV, we note that the interaction with the land surface may therefore extend beyond the regions identified as first-order continental moisture sources.

4.5 Factors governing local recycling

Local recycling refers to the evaporation within a region contributing to precipitation within the region itself. Local recycling is therefore a subset of continental recycling (Fig. 6). For the YRV, the local recycling peaks in August (Fig. 9a), a time when contributions from all other sources except the Western Pacific have decreased compared to earlier months (Fig. 5e). Local recycling in the YRV is thus important for sustaining precipitation in the later part of the summer monsoon. YRV precipitation is lower in August compared to June–July. Thereby, increased local recycling acts against a further decrease. The fractional contribution from local recycling increases from 9.8 % in July to its highest value of 15.8 % in August. A peculiar finding is that local recycling peaks 2 months after the peak in contribution from moisture sources outside the target region (Fig. 9b, note the different scales). In this section, we investigate the possible reasons for the peak in local recycling in August by an analysis of the seasonal evolution of characteristic variables of the YRV water cycle, including ET, soil moisture, NDVI, and local wind speed.

The ET rate within the region (Fig. 9c, blue) is high when local recycling peaks in August. However, ET peaks in July, when the fraction of local recycling is still quite low. The ET rate can be important for sustaining local recycling but can not in itself explain why local recycling peaks in August. Figure 9c (green) shows the time evolution of ϵ within the YRV, the same variable as in Fig. 7b. The fraction of recycled ET is relatively stable throughout the year, except for the months of July, December, and January. During 9 months of the year, including August, approximately 12.7 % of ET in the region returns as precipitation. In July, this part is reduced to 9.5 %.

The soil moisture in the region (Fig. 9d, pink) also shows a seasonality distinct to local recycling. The gradual increase

Table 2. Second-order moisture sources to YRV.

	Second-order land contribution/ 10^{12} kg d $^{-1}$	Percent of YRV precipitation recycled more than once	Percent of YRV precipitation recycled once only	Percent of YRV precipitation directly from ocean sources
April–May	1.87	47.9 %	16.1 %	36.0 %
June–July	1.70	37.7 %	20.4 %	41.9 %
August–September	1.02	35.9 %	15.3 %	48.8 %
Wet season mean	1.53	40.8 %	17.6 %	41.6 %
All year	1.23	42.7 %	16.4 %	41.9 %

Table 3. Local variables for the five driest (1981, 1985, 2003, 2006, 2013) and wettest (1993, 1995, 1996, 1998, 1999) YRV summers.

	Driest five		Average	Wettest five	
Moisture supply/precipitation ($\times 10^{12}$ kg d^{-1})	3.12	−22.2 %	4.02	5.14	+28.0 %
YRV contribution ($\times 10^{11}$ kg d^{-1})	4.00	−6.12 %	4.27	4.46	+4.62 %
Local recycling	13 %		11 %	9 %	
ET (mm d^{-1})	3.8	+4 %	3.6	3.5	−5 %
Soil moisture (m^3 m^{-3})	0.2714	−3.6 %	0.2818	0.2950	+4.7 %
NDVI*	0.47	+2.6 %	0.46	0.46	−1.2 %
Wind speed (m s^{-1})	5.8	−4.8 %	6.1	6.7	+10.2 %

* NDVI data only included for years between 1982 and 2015.

in soil moisture from January to July can not explain the abrupt increase in the local recycling fraction from July to August. Since local recycling lags 2 months behind the precipitation peak, we explored the possibility that moisture from June or July precipitation was stored in the soil and affected August local recycling. However, interannual correlations of June or July soil moisture with local recycling in August are close to zero, both for absolute values of moisture contribution and the fraction of local recycling (not shown). We recognize that the soil moisture may participate in causing the late peak in local recycling but is not a driving factor.

The NDVI is a satellite-observed index for the density of green leaves (Pinzon and Tucker, 2014). The NDVI average over the region shows a gradual increase from January onward (Fig. 9d). NDVI peaks in August and stays high in September, similar to the local recycling fraction. This means vegetation and moisture released through transpiration could help support the local recycling peak in August and perseverance in September.

Finally, to compare local recycling with the circulation in the region, we used the 850 hPa mean wind speed over the YRV as an index (Fig. 9e). The wind speed over the region has a marked peak in July, concurrent with the decrease in recycled ET (Fig. 9c). The stronger winds in July advect more moisture from distant sources, as well as a potentially stronger export of locally evaporated moisture. In contrast, weaker winds can increase the chances of locally evaporated moisture re-precipitating within the region during August and subsequent months. At the time of the local re-

cycling peak the region experiences some of the lowest wind speeds during the year, favoring higher local recycling rates.

In summary, the comparison between local recycling and characteristic variables of the water cycle in the YRV suggests that a combination of factors is responsible for causing the late peak in local recycling and maintaining late monsoon-season rainfall. Decreasing winds, high soil moisture, high green leaf area, and high evaporation rates in combination lead to a sharp rise in local recycling and a slowed decline in rainfall seasonality in August. This suggests that rainfall variability in the late monsoon season is potentially affected by each of these factors, requiring a system-oriented approach to understanding variability of the YRV hydrological cycle.

4.6 Interannual variability of local recycling and distant contribution in summer

To explore the effects of local factors on the interannual variability of moisture sources, we now focus on the five driest and wettest summers out of the 37 summers between 1980 and 2016 (Table 3). Four of the five driest and wettest years in ERA-Interim are matched by WaterSip as the most extreme. For all summers (JJA) the YRV average WaterSip precipitation estimate is 1.31 mm d^{-1} lower than in ERA-Interim. The WaterSip summer precipitation deviations range from −4 % to −33 %, with an average of 20.5 %. This is a typical bias for Lagrangian diagnostics (Sodemann et al., 2008).
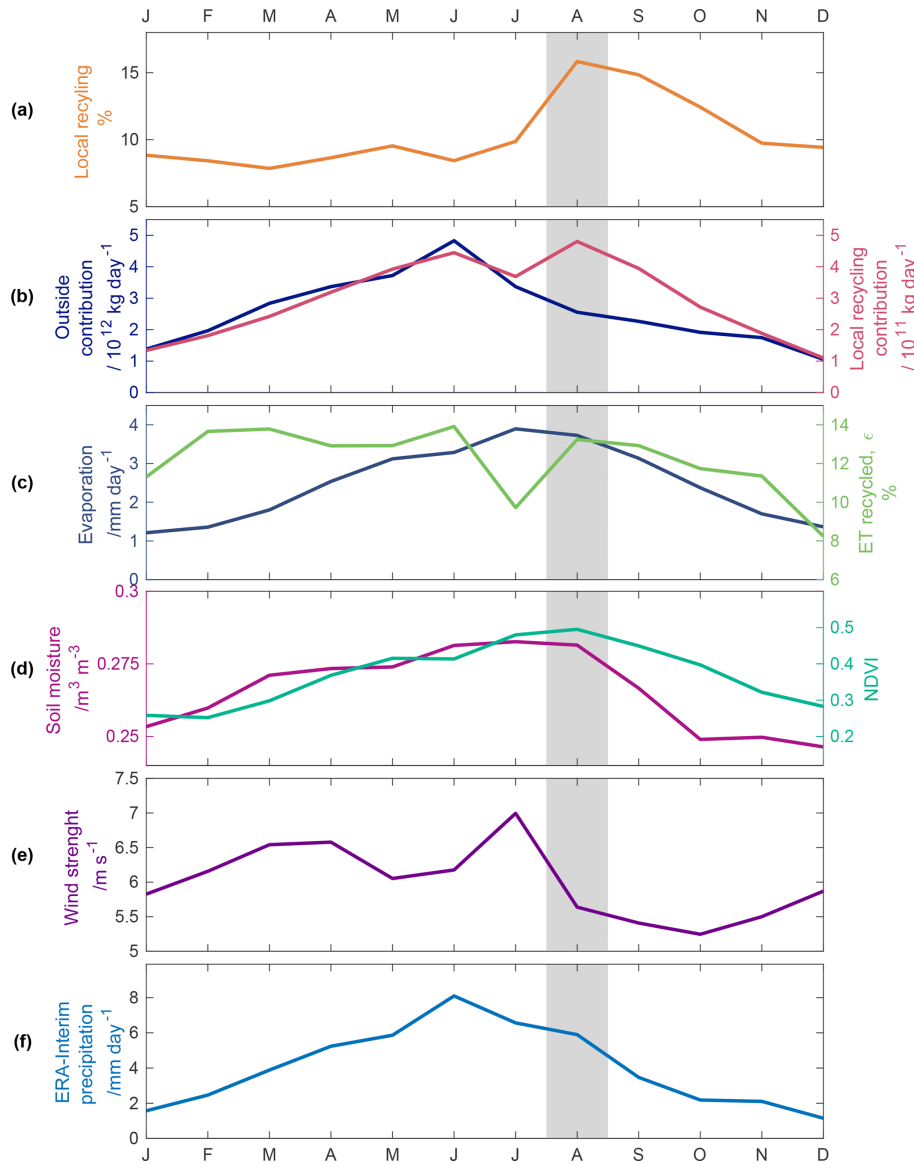
Figure 9. Seasonal cycle of YRV variables. The panels show **(a)** local recycling in percent; **(b)** absolute values of moisture contribution from regions outside YRV and within YRV in 10^{12} and 10^{11} kg d^{-1} respectively; **(c)** ERA-Interim evapotranspiration over the YRV in millimeters per day (mm d^{-1}) and ϵ, the percentage of evapotranspiration over the YRV which is recycled; **(d)** ERA-Interim soil moisture in cubic meter water per cubic meter volume (m^3 m^{-3}) and NDVI (unitless); **(e)** ERA-Interim 850 hPa wind strength over the region in meters per second (m s^{-1}); and **(f)** ERA-Interim precipitation in millimeters per day (mm d^{-1}). All values are monthly climatologies for 1980–2016 except NDVI, which is the 1982–2015 climatology. August is shaded, showing the month of the local recycling peak.

The total moisture supplied from all sources reflects the precipitation of the region, with anomalies of −22 % and +28 % during dry and wet years respectively. The relative changes in local variables are smaller (Table 3). YRV contribution is higher during wet than during dry summers. However, during wet summers the local recycling fraction is lower, suggesting that during wet summers the contribution from outside the region increases more than local contributions. Local ET, soil moisture, and NDVI all change less than 5 % in wet and dry summers compared to the mean.

The 850 hPa wind speed over the region shows the largest changes, with 10 % higher wind speeds for wet summers compared to the average and 5 % lower wind speeds during dry summers. The lower fraction of local recycling for wet summers and the high changes in wind speeds over the region suggest that outside contribution is more strongly connected to YRV precipitation variability than local moisture sources.

The small differences in local recycling between dry and wet summers motivate a comparison of moisture contribution from the different source regions for the five driest and
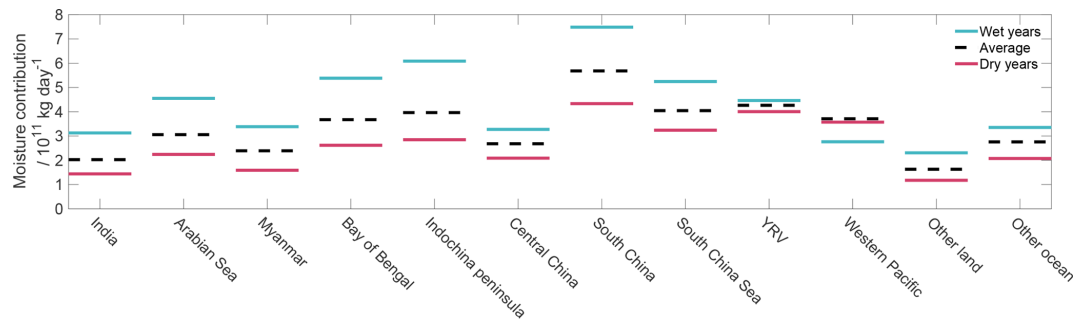
Figure 10. Moisture contribution during the five driest (1981, 1985, 2003, 2006, 2013) and wettest (1993, 1995, 1996, 1998, 1999) summers. The average contribution for all summers is also shown with dashed lines. The extent of the source regions is defined in Fig. 4.

wettest summers (Fig. 10). Contribution from all sources except the Western Pacific follow the same pattern, contributing more than average in wet summers and less than average in dry summers. The Western Pacific breaks the pattern and provides the least moisture for wet summers and slightly less than average in dry summers. The changes between contribution in dry and wet summers are smallest for the YRV. This suggests that the YRV has a more stable contribution to summer precipitation than sources outside the domain and that contribution from the YRV does not intensify interannual variability. The largest changes in contribution between dry and wet summers are seen for South China and the Indochina Peninsula. South China provides -24% during dry summers and $+32\%$ during wet summers compared to its average summer contribution. The Indochina Peninsula provides -28% and $+53\%$ in dry and wet summers respectively. As these two land regions contribute a large fraction (24 %) of summer precipitation moisture, their variability also plays a large role in the interannual variability of YRV moisture sources and precipitation.

The South China Sea is the ocean region providing the largest amount of moisture in summer ($4.0 \times 10^{11}\,\mathrm{kg\,d^{-1}}$), and the Western Pacific provides the second largest amount ($3.7 \times 10^{11}\,\mathrm{kg\,d^{-1}}$). However, neither of these show the largest changes in contribution between dry and wet summers. The largest absolute changes between dry and wet years occur for the Indian Ocean sources of the Bay of Bengal (2.6 to $5.4 \times 10^{11}\,\mathrm{kg\,d^{-1}}$) and the Arabian Sea ($2.2$ to $4.5 \times 10^{11}\,\mathrm{kg\,d^{-1}}$). The South China Sea is next (3.2 to $5.2 \times 10^{11}\,\mathrm{kg\,d^{-1}}$). The Indian Ocean sources therefore seem to play the largest role for the interannual variability of YRV moisture sources and precipitation, with the South China Sea following slightly behind.

Guo et al. (2018) previously found that the major contributors of moisture influxes to different regions of China are not necessarily the major contributors to precipitation interannual variability. We arrive to a similar conclusion, although different study regions and methods hinder a direct comparison of our results. According to our findings, South China, the Indochina Peninsula, and the Indian Ocean contribute the

most to YRV summer precipitation interannual variability. On the other hand, the YRV region, the South China Sea, and the Western Pacific, which are some of the major moisture sources, contribute less to interannual variability.

5 Discussion

Based on the view of what constitutes a moisture source, previous studies on the moisture sources of the YRV can be divided into three groups. First, there are those that mainly consider ocean sources, which result in finding the most important ocean moisture sources (Zhou and Yu, 2005; Zhou et al., 2010; Wang and Chen, 2012). While knowledge of the ocean moisture sources is valuable, and one can argue that all moisture eventually comes from the ocean, it is first by including land sources in the analysis that we get the possibility to uncover the role of the land surface for moisture source variability.

The second group of studies estimated moisture sources as the net $e - p$ in the history of an air parcel (Chen et al., 2013; Li et al., 2016; Drumond et al., 2011). This view on moisture sources, while practical for finding net sources and sinks, has several drawbacks. The dominance of p over e in a 10 d integral map can mask the process of continental recycling, leading to the underestimation of land sources. In addition, to prescribe equal significance to all moisture changes in a trajectory's history causes a high dependency on the choice of trajectory length. Results from the $e - p$ method will not show the last place of evaporation for YRV precipitation.

Finally, there are a set of studies which, like this study, search for the regions where the moisture of a precipitation event last evaporated. A range of methods have been used, all with their separate advantages and disadvantages. The study of Wei et al. (2012) was based on the quasi-isentropic back-trajectory method (Dirmeyer and Brubaker, 2007), Sun and Wang (2015) used FLEXPART trajectories and an accounting method along trajectories similar to this study. The study of Zhao et al. (2016) was based on the column water accounting method of van der Ent et al. (2010). Rodríguez et al. (2017) was based on a Met Office Unified Model climate

simulation, and Pan et al. (2017) was based on a simulation with the climate model CAM5.1 and the MERRA reanalysis data. Although this last group of studies is based on different data sources and examines slightly different regions, they all support that land is among the most important moisture source regions to the YRV and surrounding regions, with the Indian Ocean providing an important part of the moisture for the monsoon precipitation peak and large seasonal variations between contributions from different regions. Based on the location of the moisture sources and the seasonal cycle, the study of Rodríguez et al. (2017) and that of Pan et al. (2017) showed the most similarities to our results. As this study used a very different method to these, we conclude that these results are the most reliable.

The method we have used in this study involving FLEXPART and WaterSip brings its own set of uncertainties. To be able to distinguish evaporation from precipitation events, the method assumes that either evaporation or precipitation dominates within each time step of 6 h and disregards the other (Sodemann et al., 2008). The choice of trajectory length can influence the ability to find a source for a precipitation event (Sodemann and Stohl, 2009). A threshold for minimum moisture uptake and release from an air parcel is set to try to deal with numerical errors. This threshold also deals with the effect of air parcels mixing and thus introducing incorrect moisture sources. The threshold of minimum relative humidity for target region precipitation is the most influential threshold and can affect the estimated precipitation over the target region if changed. Ultimately, the results are limited by the ability of ERA-Interim to represent the actual state of the atmosphere.

When choosing a method to answer a research question, the definition of what constitutes a moisture source leads to large differences in results and should be considered carefully. Still, for the methods with similar views on the definition of moisture sources, results are difficult to compare directly. It would be beneficial to have a common measure to compare the different results. For example, the summer mass-average moisture source distance for our results is 2420 km with a monthly standard deviation of ±376 km. The mass-average moisture source distance describes the distance between all moisture source evaporation events and the corresponding target region precipitation events, weighted by their contribution to precipitation in the target area. This is equivalent to the distance between the centroid of the moisture sources. The centroid of the moisture sources in our results is located at $19 \pm 2°$ N and $100 \pm 7°$ E. Using these variables, future studies may be able to quantitatively compare their results to our present findings.

6 Conclusions

The Yangtze River valley (YRV) is under the influence of the East Asian monsoon, which causes dry winters and wet
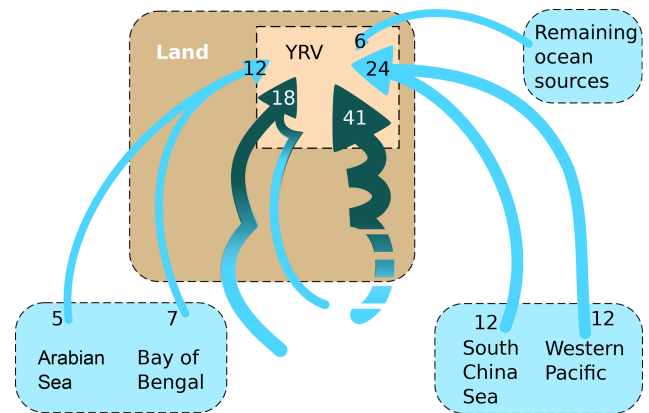
Figure 11. Moisture sources of the YRV during April–September. All numbers are contributions expressed as the percentage of YRV precipitation. Light blue arrows represent direct ocean contribution, while light-to-dark arrows represent oceanic moisture with unknown origin recycled once (left) or more than once (right) before precipitating over the YRV.

summers. In addition to large seasonal variations, the YRV also experiences large interannual variability. As a way to decipher the underlying mechanisms for precipitation variability, we have studied the variability of YRV precipitation moisture sources using the ERA-Interim reanalysis dataset for the years 1980–2016. Trajectories from the Lagrangian model FLEXPART were used in combination with the moisture source diagnostic tool WaterSip to quantify the moisture sources. Thereby, we take a perspective that allows for both continental and oceanic sources of moisture. The ocean was found to directly contribute 42 % of moisture for precipitation in the YRV (Fig. 11). Furthermore, the ocean contributes moisture indirectly through the means of continental recycling. Continental recycling allows the land surface to supply 58 % of moisture for precipitation, where one-third is ocean moisture recycled on land once before precipitating over the YRV, while two-thirds are recycled on land more than once. According to our results, land moisture sources by means of continental recycling provide more than half of the precipitation in the YRV. Hence, factors at the land surface such as evapotranspiration, soil moisture, and vegetation are likely to influence moisture source contributions.

The key results of this study are summarized below:

- Continental moisture sources supplied a large part (58.4 %) of the moisture for the YRV precipitation. At first sight this number might seem surprisingly high. However, comparing with reanalysis evapotranspiration rates at the source regions we showed that results were in a reasonable range.

- Ocean moisture sources contributed 41.6 % of moisture for YRV precipitation directly and contributed more moisture indirectly by means of continental recycling.

– Local recycling provides moisture for YRV precipitation from within the region. Local recycling peaks 2 months after the monsoon precipitation peak and constitutes 15.8 % in August.

– The intraseasonal variability of local recycling is related to a combination of the factors evapotranspiration, soil moisture, vegetation, and 850 hPa wind speed in the YRV. Wind speed thereby appears as one of the main factors and could likely explain the late peak in local recycling.

– The second-order sources of the YRV precipitation consist of 17.6 % ocean moisture which was recycled on land once, while 40.8 % was recycled on land more than once. Results for second-order sources showed how land source regions receive moisture from a mix of land and ocean sources.

– Moisture sources for the five driest and wettest summers in the YRV are most closely connected to interannual variability of the ocean sources of the Bay of Bengal and the Arabian Sea, as well as the continental sources of the Indochina Peninsula and South China. On the other hand, the South China Sea, the Western Pacific, and the YRV region itself, while important for providing moisture in the climatology, are less important when it comes to interannual variability.

The results of this study support the view that land regions in a larger region of East Asia are critically important for moisture supply and precipitation variability of the YRV. This study also emphasizes that a different set of land and ocean moisture sources are important for sustaining the summer climatology, causing intraseasonal variability and interannual variability. This view serves as an important backdrop for understanding how land–atmosphere interactions influence YRV precipitation in past, present, and future climates.

Code and data availability. The code and data used in this study are available from the authors on request.

Author contributions. AF and HS designed the study, performed the analysis, and wrote the manuscript jointly.

Competing interests. The authors declare that they have no conflict of interest.

References

Baker, A., Sodemann, H., Baldini, J., Breitenbach, S., Johnson, K., van Hunen, J., and Zhang, P.: Seasonality of westerly moisture transport in the East Asian summer monsoon and its implications for interpreting precipitation δ^{18}O, J. Geophys. Res.-Atmos., 120, 5850–5862, https://doi.org/10.1002/2014JD022919, 2015.

Chen, B., Xu, X.-D., and Zhao, T.: Main moisture sources affecting lower Yangtze River Basin in boreal summers during 2004–2009, Int. J. Climatol., 33, 1035–1046, https://doi.org/10.1002/joc.3495, 2013.

Chen, L., Chen, D., Wang, H., and Yan, J.: Regionalization of Precipitation Regimes in China, Atmos. Ocean. Sci. Lett., 2, 301–307, https://doi.org/10.1080/16742834.2009.11446818, 2009.

Dee, D. P., Uppala, S. M., Simmons, A. J., Berrisford, P., Poli, P., Kobayashi, S., Andrae, U., Balmaseda, M. A., Balsamo, G., Bauer, P., Bechtold, P., Beljaars, A. C. M., van de Berg, L., Bidlot, J., Bormann, N., Delsol, C., Dragani, R., Fuentes, M., Geer, A. J., Haimberger, L., Healy, S. B., Hersbach, H., Holm, E. V., Isaksen, L., Kallberg, P., Kohler, M., Matricardi, M., McNally, A. P., Monge-Sanz, B. M., Morcrette, J. J., Park, B. K., Peubey, C., de Rosnay, P., Tavolato, C., Thepaut, J. N., and Vitart, F.: The ERA-Interim reanalysis: configuration and performance of the data assimilation system, Q. J. Roy. Meteorol. Soc., 137, 553–597, https://doi.org/10.1002/qj.828, 2011.

Ding, Y. H. and Chan, J. C. L.: The East Asian summer monsoon: an overview, Meteorol. Atmos. Phys., 89, 117–142, https://doi.org/10.1007/s00703-005-0125-z, 2005.

Dirmeyer, P. A. and Brubaker, K. L.: Characterization of the global hydrologic cycle from a back-trajectory analysis of atmospheric water vapor, J. Hydrometeorol., 8, 20–37, https://doi.org/10.1175/JHM557.1, 2007.

Drumond, A., Nieto, R., and Gimeno, L.: Sources of moisture for China and their variations during drier and wetter conditions in 2000–2004: a Lagrangian approach, Clim. Res., 50, 215–225, https://doi.org/10.3354/cr01043, 2011.

Feng, X. U. E., Zeng, Q., Huang, R., Li, C., Lu, R., and Zhou, T.: Recent Advances in Monsoon Studies in China, Adv. Atmos. Sci., 32, 206–229, https://doi.org/10.1007/s00376-014-0015-8, 2015.

Goessling, H. F. and Reick, C. H.: What do moisture recycling estimates tell us? Exploring the extreme case of non-evaporating continents, Hydrol. Earth Syst. Sci., 15, 3217–3235, https://doi.org/10.5194/hess-15-3217-2011, 2011.

Guo, L., Klingaman, N. P., Demory, M. E., Vidale, P. L., Turner, A. G., and Stephan, C. C.: The contributions of local and remote atmospheric moisture fluxes to East Asian pre-

cipitation and its variability, Clim. Dynam., 51, 4139–4156, https://doi.org/10.1007/s00382-017-4064-4, 2018.

Huang, D. Q., Zhu, J., Zhang, Y. C., Huang, Y., and Kuang, X. Y.: Assessment of summer monsoon precipitation derived from five reanalysis datasets over East Asia, Q. J. Roy. Meteorol. Soc., 142, 108–119, https://doi.org/10.1002/qj.2634, 2016.

Huang, R., Chen, J., and Huang, G.: Characteristics and Variations of the East Asian Monsoon System and Its Impacts on Climate Disasters in China, Adv. Atmos. Sci., 24, 993–1023, https://doi.org/10.1007/s00376-007-0993-x, 2007.

Huang, R., Chen, J., Wang, L., and Lin, Z.: Characteristics, processes, and causes of the spatio-temporal variabilities of the East Asian monsoon system, Adv. Atmos. Sci., 29, 910–942, https://doi.org/10.1007/s00376-012-2015-x, 2012.

Jun, X. and Chen, Y. D.: Water problems and opportunities in the hydrological sciences in China, Hydrolog. Sci. J., 46, 907–921, https://doi.org/10.1080/02626660109492885, 2001.

Läderach, A. and Sodemann, H.: A revised picture of the atmospheric moisture residence time, Geophys. Res. Lett., 43, 924–933, https://doi.org/10.1002/2015GL067449, 2016.

Li, L., Dolman, A. J., and Xu, Z.: Atmospheric moisture sources, paths, and the quantitative importance to the Eastern Asian Monsoon region, J. Hydrometeorol., 17, 637–649, https://doi.org/10.1175/JHM-D-15-0082.1, 2016.

Lin, R., Zhou, T., and Qian, Y.: Evaluation of Global Monsoon Precipitation Changes based on Five Reanalysis Datasets, J. Climate, 27, 1271–1289, https://doi.org/10.1175/JCLI-D-13-00215.1, 2014.

Liu, Z., Liu, Y., Wang, S., Yang, X., Wang, L., Baig, M. H. A., Chi, W., and Wang, Z.: Evaluation of spatial and temporal performances of ERA-interim precipitation and temperature in Mainland China, J. Climate, 31, 4347–4365, https://doi.org/10.1175/JCLI-D-17-0212.1, 2018.

Pan, C., Zhu, B., Gao, J., and Kang, H.: Source apportionment of atmospheric water over East Asia – a source tracer study in CAM5.1, Geosci. Model Dev., 10, 673–688, https://doi.org/10.5194/gmd-10-673-2017, 2017.

Piao, S., Ciais, P., Huang, Y., Shen, Z., Peng, S., Li, J., Zhou, L., Liu, H., Ma, Y., Ding, Y., Friedlingstein, P., Liu, C., Tan, K., Yu, Y., Zhang, T., and Fang, J.: The impacts of climate change on water resources and agriculture in China, Nature, 467, 43–51, https://doi.org/10.1038/nature09364, 2010.

Pinzon, J. E. and Tucker, C. J.: A Non-Stationary 1981–2012 AVHRR NDVI3g Time Series, Remote Sensing, 6, 6929–6960, https://doi.org/10.3390/rs6086929, 2014.

Rodríguez, J. M., Milton, S. F., and Marzin, C.: The East Asian Atmospheric Water Cycle and Monsoon Circulation in the Met Office Unified Model, J. Geophys. Res.-Atmos., 122, 10246–10265, https://doi.org/10.1002/2016JD025460, 2017.

Sodemann, H. and Stohl, A.: Asymmetries in the moisture origin of Antarctic precipitation, Geophys. Res. Lett., 36, 1–5, https://doi.org/10.1029/2009GL040242, 2009.

Sodemann, H., Schwierz, C., and Wernli, H.: Interannual variability of Greenland winter precipitation sources: Lagrangian moisture diagnostic and North Atlantic Oscillation influence, J. Geophys. Res.-Atmos., 113, D03107, https://doi.org/10.1029/2007jd008503, 2008.

Stohl, A. and James, P.: A Lagrangian analysis of the atmospheric branch of the global water cycle. Part I: Method description, validation, and demonstration for the August 2002 flooding in central Europe, J. Hydrometeorol., 5, 656–678, https://doi.org/10.1175/1525-7541(2004)005<0656:ALAOTA>2.0.CO;2, 2004.

Stohl, A. and Thomson, D. J.: A Density Correction for Lagrangian Particle Dispersion Models, Bound.-Lay. Meteorol., 90, 155–167, https://doi.org/10.1023/A:1001741110696, 1999.

Stohl, A., Hittenberger, M., and Wotawa, G.: Validation of the Lagrangian particle dispersion model FLEXPART against large-scale tracer experiment data, Atmos. Environ., 32, 4245–4264, https://doi.org/10.1016/S1352-2310(98)00184-8, 1998.

Stohl, A., Forster, C., Frank, A., Seibert, P., and Wotawa, G.: Technical note: The Lagrangian particle dispersion model FLEXPART version 6.2, Atmos. Chem. Phys., 5, 2461–2474, https://doi.org/10.5194/acp-5-2461-2005, 2005.

Stohl, A., Forster, C., and Sodemann, H.: Remote sources of water vapor forming precipitation on the Norwegian west coast at 60° N – A tale of hurricanes and an atmospheric river, J. Geophys. Res.-Atmos., 113, 1–13, https://doi.org/10.1029/2007JD009006, 2008.

Sun, B. and Wang, H.: Analysis of the major atmospheric moisture sources affecting three sub-regions of East China, Int. J. Climatol., 35, 2243–2257, https://doi.org/10.1002/joc.4145, 2015.

Sun, Q., Miao, C., and Duan, Q.: Extreme climate events and agricultural climate indices in China: CMIP5 model evaluation and projections, Int. J. Climatol., 36, 43–61, https://doi.org/10.1002/joc.4328, 2016.

van der Ent, R. J., Savenije, H. H. G., Schaefli, B., and Steele-Dunne, S. C.: Origin and fate of atmospheric moisture over continents, Water Resour. Res., 46, W09525, https://doi.org/10.1029/2010WR009127, 2010.

van der Ent, R. J., Wang-Erlandsson, L., Keys, P. W., and Savenije, H. H. G.: Contrasting roles of interception and transpiration in the hydrological cycle – Part 2: Moisture recycling, Earth Syst. Dynam., 5, 471–489, https://doi.org/10.5194/esd-5-471-2014, 2014.

Wang, H. and Chen, H.: Climate control for southeastern China moisture and precipitation: Indian or East Asian monsoon?, J. Geophys. Res.-Atmos., 117, D12109, https://doi.org/10.1029/2012jd017734, 2012.

Wei, J., Dirmeyer, P. A., Bosilovich, M. G., and Wu, R.: Water vapor sources for Yangtze River Valley rainfall: Climatology, variability, and implications for rainfall forecasting, J. Geophys. Res.-Atmos., 117, D05126, https://doi.org/10.1029/2011JD016902, 2012.

Wu, J. and Gao, X.: A gridded daily observation dataset over China region and comparison with the other datasets, Chinese J. Geophys., 56, 1102–1111, https://doi.org/10.6038/cjg20130406, 2013.

Zhao, T., Zhao, J., Hu, H., and Ni, G.: Source of atmospheric moisture and precipitation over China's major river basins, Front. Earth Sci., 10, 159–170, https://doi.org/10.1007/s11707-015-0497-4, 2016.

Zhou, T. J. and Yu, R. C.: Atmospheric water vapor transport associated with typical anomalous summer rainfall patterns in China, J. Geophys. Res.-Atmos., 110, D08104, https://doi.org/10.1029/2004JD005413, 2005.

Zhou, X., Ding, Y., and Wang, P.: Moisture Transport in the Asian Summer Monsoon Region and Its Relationship with Summer Precipitation in China, Acta Meteorol. Sin., 24, 31–42, 2010.